75th International Astronautical Congress (IAC), Milan, Italy, 14-18 October 2024.

IAC-24-A3.5.7

Real time data-based wind model for a Venus Aerobot: development and testing

Camilla Bandinelli[a]*, Elisa Capello[a], Ashish Goel[b], Federico Rossi[b], Marco B. Quadrelli[b]

[a] *Department of Mechanical and Aerospace Engineering, Politecnico of Torino, Torino, Italy*
[b] *Jet Propulsion Laboratory, California Institute of Technology, 4800 Oak Grove Drive, Pasadena, CA, 91109-8099 – U.S.A.*
* Corresponding Author

Abstract

The surface of Venus is characterized by extreme temperature and a crushing pressure. However, at altitudes between 51 to 62 km, conditions resemble Earth's surface, making it an ideal location for a proposed mission concept that involves deploying a balloon with a suspended science gondola, known as an aerobot. Due to the planet's extreme wind conditions, with gusts reaching up to 100 m/s, and the complexities of balloon dynamics in the atmosphere, detailed models of wind gusts are critical to predict the aerobot's dynamics. Unfortunately, previous missions have only collected surface wind data and vertical gusts, leaving horizontal gusts data missing.
The goal of this paper is to present the development of a systematic method to generate wind gust model capable of capturing the highly non-stationary and random characteristics of wind gusts from real-time data. The model is fitted to data collected during terrestrial flight tests, so it can be used in predictive simulations of the Venus aerobot behavior in Earth field experiments. The proposed approach relies on a set of stochastic differential equations, specifically a bidimensional Ornstein-Uhlenbeck process, to accurately represent the autocorrelation function and probability density function of a measured wind signal. The first function captures the "memory effect" of the signal, while the second one serves as a tool for reproducing the observed instantaneous distribution of wind direction and speed.
The proposed method was tested using real-world wind speed measurement data collected by Jet Propulsion Laboratory during flight tests in the Mojave Desert. An extended Kalman filter was used to process the real-time wind signal captured by measurement instruments before incorporating it into the model. This filter adeptly captures the dynamics of an atmospheric balloon, and efficiently fuses data from inertial measurement units and wind measurement instruments.
Results indicate that the proposed method is simple to implement and can accurately capture simultaneously the autocorrelation and probability distribution of wind speed measurement data, and holds promise as a tool for design of future Venus aerobots.

Keywords: Stochastic Wind Gust Model, Venus Atmosphere, Aerobot, Balloon, Extended Kalman Filter

Acronyms/Abbreviations

ACF	Autocorrelation Function
ARMA	Autoregressive Moving Average
BCM	Buoyancy Control Module
CDF	Cumulative Distribution Function
ECDF	Empirical Cumulative Distribution Function
EKF	Extended Kalman Filter
IMU	Inertial Measurement Unit
INS	Inertial Navigation System
JPL	Jet Propulsion Laboratory
OU	Ornstein-Uhlenbeck
PDF	Probability Density Function
RMSE	Root Mean Squared Error
SDE	Stochastic Differential Equation

1. Introduction

1.1 Motivation

Venus is the nearest planet to the Earth, observed since ancient times as the beautiful, brilliant morning or evening 'star' in the night sky. Venus is also the celestial body most similar to ours in size, mass and composition. The planet has an especially thick carbon dioxide atmosphere, which creates, together with its global sulfuric acid cloud cover, an extreme greenhouse effect. This results at the surface in a mean temperature of 464°C and a crushing pressure of 92 times that of Earth's at sea level, turning the air into a supercritical fluid. However, at altitudes between 51 to 62 km above the surface where

clouds are located, the pressure, temperature, and radiation are similar to those at Earth's surface [1], with recent research having found suggestive, but not definitive, evidence of the biomarker phosphine, possible evidence of life. Venus may have had liquid surface water early in its history, possibly enough to form oceans.

The recent selection of two Venus orbiters, NASA's VERITAS (Venus Emissivity, Radio Science, InSAR, Topography, and Spectroscopy) and ESA's EnVision, as well as NASA's DAVINCI (Deep Atmosphere Venus Investigation of Noble gases, Chemistry, and Imaging) entry probe, will fulfill many of the objectives sought by the NASA Venus science community. However, the subsequent 2023-2032 Planetary Science and Astrobiology Decadal Survey notes that other Venus science objectives remain largely unaddressed by these missions, fundamentally because they require long duration in-situ measurements from within the atmosphere [2].

Due to environmental constraints on the planet, landed surface missions are confronted with unique technological hurdles. Conversely, aerial platforms operating within the cloud layer can provide in-situ access within the atmosphere under more favorable thermal conditions. This has motivated a strong technology development focus on Venus aerial platforms at NASA's Jet Propulsion Lab (JPL).

A recent NASA-sponsored study on Venus Aerial platforms found that aerial platforms that can control altitude occupy the sweet spot in the trade space, and that there are no technology show-stoppers to their adoption for future NASA missions [3]. Specifically, long-duration variable altitude balloons based on lighter-than-air vehicle technology seem to be a highly promising solution. These vehicles consume electrical power to change altitude via gas pumping, instead of traditional balloon techniques of ballast drops and venting of buoyancy gas that permit flights of only limited duration before exhausting the consumables. This application tends to be more interested in the ability of the balloon to scientifically explore a wide range of altitudes in the clouds as compared to current terrestrial balloons that use altitude control mostly as a means to effect trajectory control, which is challenging in Venus atmosphere. Furthermore, balloon platforms have operated on Venus before [4]: the Soviet VeGa missions included two small 7 kg balloon probes that flew for approximately 48 hours in the cloud layer.

The term "aerobot," which combines the words "aeronautical" and "robot," is used to describe a robotic balloon vehicle that autonomously exercises trajectory and/or altitude control. In this paper, the term "aerobot" will be used to refer to the complete robotic vehicle, which comprises the balloon, payloads (mounted on a platform designated as a gondola), and tethers.

Venus exhibits a distinctive vertical wind profile, characterized by predominantly east-to-west zonal winds between altitudes of approximately 10-100 km. These zonal winds intensify with altitude from 10 to 65-70 km, peaking at speeds around 100 m/s at 65 km, generating horizontal wind gusts [5].

The aerobot, characterized only by a vertical control of the motion, navigates through the atmosphere propelled by zonal winds, which determine its horizontal trajectory and carry the vehicle around the planet in approximately 5 to 6 Earth-days. Additionally, the wind patterns influence the dynamics of the gondola, suspended under the balloon by means of tethers, potentially causing torsional effects which excite the payload dynamics.

Several numerical models ([6,7]) are available to simulate atmospheric circulation on Venus, largely derived from the legacy of Pioneer Venus and subsequent soviet Venera missions, and images from Venus Express, has provided three-dimensional wind speed maps at various altitudes within the cloud layer [8]. However, none of the missions that have ventured into the planet's atmosphere have recorded in-situ continuous wind speed measurements. Accordingly, stochastic, physics-based wind models that are representative of typical planetary winds that a balloon might encounter are required for the design of future Venus aerobots.

1.2 Literature review

A wide range of wind speed models are available in the literature for Earth applications, primarily focusing on wind speed forecasting and modeling forecast errors. Discrete Autoregressive Moving Average (ARMA) models are the most common and have been widely used for short-term forecasting [10,11]. Additionally, first-order and higher-order Markov chains have been extensively used to model wind speed [12,13], including applications in planetary exploration [14]. Physical models that use meteorological information have also been employed for long-term wind speed prediction [10], though they are not applicable in this context.

Both ARMA models and Markov chains are discrete in time and require a fixed time step that matches the sampling interval of the available data. This constraint limits their use in transient stability analysis for an aerobot, which involves assessing the dynamic response to rapid changes in wind conditions. Discrete models, with their fixed time intervals, may not capture these fast variations accurately, potentially compromising the precision of the analysis. Therefore, continuous wind speed models are often preferable, as they can provide the necessary high temporal resolution and responsiveness for effective transient stability assessment. Although methods exist to define a continuous-time equivalent of ARMA models, these procedures introduce numerical approximations and

require complex modeling, further affecting the precision needed for detailed dynamic analysis of the aerobot.

In recent years, the use of stochastic differential equations (SDEs) for wind speed modeling has gained popularity. SDEs appear more suitable than classical discrete time series approaches as they are intrinsically continuous with respect to time and are not constrained to use the sampling time step of the original measurement data.

1.3 Contributions

The contribution of this work is to propose a systematic method to generate stochastic wind models based on SDEs that can generate continuous wind data and is representative of wind speed trends in the Venus's atmosphere. To achieve this, the model captures and reproduces statistical properties of real wind measurements: the autocorrelation function (ACF) and the probability density function (PDF). The ACF is a measure of how the wind speed changes over time. That is, the ACF gives a measure of the relationship between the current wind speed value and past wind speed values, introducing a memory effect. The memory effect in the model allows the historical evolution of the wind to be considered, enabling a more realistic and complete representation of its characteristics. The PDF describes the likelihood that the wind speed will assume a value within a given range.

This enables the approach to be used in in-situ applications during the mission, leveraging the wind speed data recorded by the instruments. This data can be employed to support autonomous balloon guidance techniques [9]; in addition, it can be used to support Earth-based field tests when fitted to measurements of wind speeds on Earth.

1.4 Organization

The structure of this paper is as follows: Section 2 provides an overview of key concepts related to SDEs. Section 3 introduces the theoretical framework for the proposed wind speed model synthesis method. Section 4 explains the parameter identification process for SDE models using wind speed data. Section 5 details the wind data collection and processing methods during a Earth field test, while Section 6 discusses the application of these data to validate the wind model. Lastly, Section 7 summarizes the findings and suggests avenues for future research.

2. Stochastic Differential Equation

A SDE in the Itô sense is a differential equation that describes the time evolution of random phenomena under uncertainty. It is given in the one-dimensional form as follows:

$$dX(t) = f(X(t), t)dt + L(X(t), t)dW(t) \qquad (1)$$

where the continuous functions $f(X(t), t)$ and $L(X(t), t)$ represent the so-called drift and volatility terms, respectively. The drift and diffusion terms of (1) determine the statistical properties of the variable X(t), which in our case, represents the wind speed. The building block of our model is the standard Wiener process W(t) [15], which introduces randomness into the SDE (1). The equation (1) can be expressed in integral form as follows:

$$X(t) = X(t_0) + \int_{t_0}^{t} f(X(s), s)ds + \int_{t_0}^{t} L(X(s), s)dW(s) \qquad (2)$$

where $X(t_0)$ is the initial condition which is a random variable. The first integral is an ordinary Riemann-Stieltjes integral, while the second integral is defined as the Itô stochastic integral. This is because the Wiener process cannot be integrated in the conventional Riemann-Stieltjes sense, as it is not bounded.

A comprehensive examination of SDEs is beyond the scope of this paper. For further details on the theory and numerical methods of SDEs, the interested reader is referred to Refs. [16, 17].

2.1 Ornstein-Uhlenbeck process

The Ornstein-Uhlenbeck (OU) process [18] is a special case of the stochastic process with the tendency to return to a certain (constant or time-varying) level with bounded variance around it, called mean reversion. The OU process is defined as the solution of the following SDE:

$$dX(t) = -\lambda X(t)dt + \theta dW(t) \quad (3)$$

where λ is the decay rate and measures how strongly the process responds to perturbations, and $\theta > 0$ is the size of the perturbation W(t).

This process is characterized by a normal distribution with zero mean and standard deviation $\theta^2/(2\lambda)$, and by an exponential autocorrelation whose decay rate is governed by the coefficient λ, i.e.,

$$R_X(\tau) = e^{-\lambda\tau} \quad (4)$$

where τ is the time lag.

The OU process, widely used in finance, physics, and other scientific fields, is suitable for modeling physical processes such as wind fluctuations due to its bounded variance [18].

To synthesize wind speed models, we chose to employ as the foundational building block the following 2-dimensional Ornstein-Uhlenbeck process:

$$\begin{pmatrix} dX(t) \\ dY(t) \end{pmatrix} = \begin{pmatrix} -\alpha & -\sigma \\ \sigma & -\alpha \end{pmatrix} \begin{pmatrix} X(t) \\ Y(t) \end{pmatrix} dt + \begin{pmatrix} \theta \\ 0 \end{pmatrix} dW(t) \quad (5)$$

where $\alpha > 0, \sigma > 0, \theta > 0$.

The choice of this particular process was driven by the form of the ACF linked to X(t), which can be identified by examining the covariance function of the system. Given the matrix structure in the SDE, the decay rate λ is related to the eigenvalues of the matrix $\begin{pmatrix} -\alpha & -\sigma \\ \sigma & -\alpha \end{pmatrix}$, which are:

$$\lambda_{1,2} = -\alpha \pm i\sigma \tag{6}$$

These eigenvalues indicate a complex exponential decay, where the real part −α represents the rate of exponential decay and the imaginary part σ introduces oscillatory behavior. The presence of σ means that the process will not only revert to the mean over time, but will also exhibit periodic fluctuations around this mean. Considering the eigenvalues, the ACF of X(t) can be expressed as:

$$R_X(\tau) = e^{-\alpha\tau}\cos(\sigma\,\tau) \tag{7}$$

The exponentially decaying and oscillatory nature of X(t)'s ACF is particularly suitable for modeling stochastic wind speed dynamics. Specifically:

- Exponential decay: This characteristic represents the loss of correlation over time, effectively capturing the diminishing influence of past wind speeds.
- Oscillatory behavior: This aspect reflects periodic patterns or cycles in wind speed, such as diurnal variations or regular gust patterns.

For this reason X(t) process is specifically used for constructing the wind speed model.

Note that for $\sigma = 0$, X(t) and Y(t) are decoupled and X(t) becomes a one-dimensional OU process, as in Equation (3).

3. The mathematical model

As outlined in Section 1, the objective of the model is to accurately replicate the ACF and PDF of real wind speed measurements. The process of constructing the desired compound stochastic model involves two primary steps:

- Capturing the ACF: The model uses an SDE in the form of Equation (5) to capture the desired ACF. This involves determining the appropriate coefficient values that allow the model to match the ACF of the real wind speed data. Since a single SDE may not provide an optimal fit, a weighted sum of multiple SDEs is employed to achieve a more accurate representation.
- Imposing the PDF: After defining the superposition of SDEs to capture the ACF, an analytical or numerical memoryless transformation is applied. This transformation adjusts the process to conform to the desired PDF, ensuring that the statistical properties of the modeled wind speed align with those of the observed data.

3.1 ACF modeling

Using a weighted sum of multiple SDEs in the form of (7) can improve the fit of the resulting wind model, capturing multi-modal effects with different time scales and velocity distributions. Accordingly, the proposed stochastic process comprises a weighted sum of SDEs, as follows:

$$F(t) = \sum_{i=1}^{n} \sqrt{\omega_i} X_i(t) \tag{8}$$

where $X_i(t)$ are processes with ACF in the form of (7) and the weights $\omega_i > 0$ must be

$$\sum_{i=1}^{n} \omega_i = 1 \tag{9}$$

The ACF of the process is the weighted sum of the *n* ACFs of the *n* SDEs processes:

$$R_F(\tau) = \sum_{i=1}^{n} \omega_i R_{X_i}(\tau) \tag{10}$$

If the *n* SDEs X(t) are processes as in (5), the resulting ACF of F(t) is a weighted sum of damped sinusoidal and decaying exponential functions, that is:

$$R_F(\tau) = \sum_{i=1}^{n} \omega_i e^{-\alpha_i\tau}\cos(\sigma_i\,\tau) \quad (11)$$

If all *n* processes have an identical Gaussian PDF $\mathcal{N}(\mu_X, \theta_X)$, the stochastic process F(t) has the same Gaussian PDF $\mathcal{N}(\mu_X, \theta_X)$. If the ACF does not show a periodic behavior then $\omega_i = 0, \forall i = 1, \dots, n$.

3.2 PDF modeling

The probability density function of the wind speed is typically not Gaussian, while the process F(t) in (8) has a Gaussian PDF. To impose the target PDF of the wind speed, a memoryless transformation is applied [19]. This approach converts a standard Gaussian stochastic process into another process with a different PDF that matches the desired wind speed characteristics, while preserving the correlation structure between the data points.

This memoryless transformation is obtained by applying the Gaussian cumulative distribution function (CDF) $\phi(\cdot)$ to the inverse CDF of wind data $Z^{-1}(\cdot)$:

$$F_Z(t) = Z^{-1}\left(\phi\left(F(t)\right)\right) \tag{12}$$

The resulting process is the target SDE with the desired PDF and ACF.

4. Model implementation

4.1 ACF fitting

In order to characterize the autocorrelation function of wind data, a fitting procedure is employed. This procedure utilizes a non-linear regression model, which involves the optimization of coefficients representing a weighted sum of exponential and/or damped sinusoidal functions. Initially, a range of potential models with varying numbers of components is defined. Subsequently, a genetic algorithm is employed to identify an optimal initial set of coefficients for each candidate model. The ACF data is then fitted to each model using the *fitnlm* function in MATLAB, which iteratively adjusts the model coefficients to minimize the root mean squared error (RMSE) between the fitted curve and the actual ACF data. This iterative process continues until a stopping criterion based on the RMSE and R-squared values is met, ensuring an accurate representation of the ACF.

4.2 Integration of SDE

From the fitting routine, the coefficients of the most suitable model, along with the corresponding number of components, are selected to create the superposition stochastic differential equation that accurately captures the autocorrelation function of the wind data. These coefficients, comprising the weights, damping factors, and frequencies, define the dynamics of the SDE model. Subsequently, the SDE is numerically integrated over a specified time interval to generate a stochastic process F(t) that simulates the temporal evolution of the wind speed.

An analysis comparing different stochastic integration methods identified the most suitable integration technique for accurately simulating the stochastic processes underlying the wind dynamics.

The selection was based on the stability criterion of the methods [20]. The Euler-Maruyama and Exponential methods were found to be highly sensitive to initial conditions, integration step size, and integration interval. The latter two elements are crucial for reproducing the autocorrelation function. In fact, to capture the same correlation function in the generated signal, it is necessary for the integrator to allow the signal to be generated for a sufficient time for the correlation to develop and for the integration step to be smaller than the input signal sampling rate.

In contrast, Heun's method demonstrates reduced sensitivity to the previously mentioned parameters. For this reason, it has been selected as the integrator to test the model.

Furthermore, system stability is strongly determined by the characteristics of the equation itself, particularly depending on the coefficients obtained from the fit. Once the fit is performed, it is essential to study the eigenvalues of the system of two equations and eliminate any components of the overlap that have eigenvalues with positive real part.

4.3 PDF fitting

The PDF can be defined in two ways, analytically or numerically. When dealing with irregular wind speed distributions, defining the probability density function numerically is often preferred over an analytical approach. This preference arises due to the flexibility and adaptability of numerical methods in capturing complex distributions accurately.

Analytical approaches typically rely on predefined mathematical functions or models (e.g., Gaussian) to describe the PDF. However, these functions may struggle to accurately represent distributions that are irregular or have multiple peaks. In such cases, forcing an analytical function to fit the data may result in a poor representation and inaccurate predictions.

On the other hand, numerical methods, such as kernel density estimation or histogram-based approaches, offer more flexibility in capturing the intricacies of irregular distributions. These methods do not rely on predefined functional forms but instead directly estimate the PDF from the data itself. By dividing the data into bins or using kernel functions, numerical methods can provide a more faithful representation of the underlying distribution, even when it is complex.

Among the many possible numerical techniques to approximate the probability distribution of a set of measurements, the empirical cumulative distribution function (ECDF) is considered. The ECDF provides a non-parametric estimate of the CDF based directly on the observed data points. The empirical cumulative distribution function is constructed by sorting the N data points in ascending order, assigning each data point a cumulative probability of $\frac{1}{N}$, and plotting these probabilities against the corresponding sorted data values. This process results in a step function where each step increases by $\frac{1}{N}$ for each data point. To obtain an approximation of the continuous CDF, linear interpolation is applied to the ECDF.

5. Wind data

5.1 Data Collection

In July 2023, engineers at NASA's JPL conducted two high-altitude balloon launches to simulate the dynamics of the Venus Aerobot concept. The experimental setup consisted of a lower plate representing the gondola, an upper plate serving as the

buoyancy control module (BCM), and a sounding balloon. Both plates were equipped with instruments to collect data.

The payloads incorporated an array of sensors tailored for comprehensive data collection. These included a barometer, thermistors, and an inertial navigation system (INS) unit installed on each plate. The INS unit comprised a combined GPS, gyroscope, magnetometer, and accelerometer, facilitating precise tracking of the plate's motion. An experimental anemometer was deployed to measure relative wind speed using differential pressure transducers and orthogonally mounted pitot tubes. An external thermistor and an internal barometer were included to measure temperature and atmospheric pressure, respectively, allowing for air density calculations. The gondola was not airtight to permit pressure equalization. Extensive data were gathered to analyze the dynamics and configurations of the tethers between the balloon and gondola; this data can also be used to fit a wind model and validate its accuracy, as detailed next.

The launches were conducted at the Lucerne Lakebed in the Mojave Desert, California. Both balloons successfully completed their flights and were subsequently recovered. During Flight 1, the balloon ascended to an altitude of approximately 31,274 meters, while Flight 2 reached a maximum altitude of 32,084 meters.

5.2 Data processing

The procedure for computing the relative wind speed from the pressure measured by the pitot tubes and air density involves utilizing Bernoulli's equation.

The anemometer measures the difference between wind speed and the balloon's velocity. Thus, it only detects changes in wind speed relative to the balloon, not absolute wind speed. By analyzing these relative velocities, one cannot distinguish between actual wind gusts and changes due to the balloon's movement. This distinction is crucial for accurately assessing meteorological conditions. To calculate the absolute wind speed from the relative wind speed, the system's velocity must be determined. This information is provided by GPS units installed on both the gondola and the BCM. However, the civilian GPS systems used in the flights do not function above approximately 18 km in altitude, causing GPS data, including velocity, to be unavailable during high-altitude flights. Moreover, GPS technology cannot be utilized for a mission on Venus, motivating interest in the development of a GPS-free estimator.

5.2.1 *Extended Kalman Filter*

In the absence of direct velocity measurements, velocities can be derived from inertial measurement unit (IMU) recorded accelerations using an extended Kalman filter (EKF). The balloon system's nonlinear motion dynamics, especially during wind gusts, necessitate this approach. For precise state estimation, we employ a continuous-time formulation in the prediction step to accurately capture dynamic behavior, while a discrete formulation is used in the update step to match sensor sampling frequencies. This results in a Continuous-Discrete or Hybrid EKF. To determine the balloon's atmospheric movement speed, it is sufficient to filter data from the BCM's IMU, ignoring the relative dynamics between the plates caused by tethers.

The estimated states of the system include the three components of the balloon's position $\boldsymbol{x_b}$, the three components of the balloon's velocity $\dot{\boldsymbol{x}}_{\boldsymbol{b}}$, and the three components of the absolute wind velocity $\dot{\boldsymbol{x}}_{\boldsymbol{w}}$. The measurements for the state estimation include the balloon's acceleration from accelerometers, and the relative wind velocity.

The primary ascent dynamic is driven by the balloon itself, requiring a simplified 3D dynamic model where the balloon is treated as a point mass subject to external forces. These forces include the buoyancy force F_B following Archimedes' principle, aerodynamic drag forces F_D due to wind and atmospheric motion and gravitational force F_g:

$$\boldsymbol{F_B} = \rho_{air} \cdot V \cdot \boldsymbol{g} \tag{13}$$

$$\boldsymbol{F_D} = \frac{1}{2} \cdot \rho_{air} \cdot C_D \cdot S \cdot (\dot{\boldsymbol{x}}_{\boldsymbol{b}} - \dot{\boldsymbol{x}}_{\boldsymbol{w}})^2 \tag{14}$$

$$\boldsymbol{F_g} = \boldsymbol{g} \cdot \left(m_{bcm} + m_b + m_g + m_{gas}\right) \tag{15}$$

where ρ_{air} is the density of surrounding air, V is the volume of the balloon considered as a sphere of radius R, $\boldsymbol{g}$ is the gravitational acceleration, C_D is the balloon drag coefficient set to 0.47, equivalent to that of a sphere, S is the balloon's effective area perpendicular to the flow considered as a circle of radius R, m_{bcm} is the mass of the buoyancy control module plate, m_b is the mass of the balloon envelope, m_g is the mass of the gondola plate and m_{gas} is the mass of the gas inside the balloon. The linear motion of the balloon then follows Newton's law

$$\ddot{\boldsymbol{x}}_{\boldsymbol{b}} = \frac{\boldsymbol{F_B} - \boldsymbol{F_D} - \boldsymbol{F_g}}{m_{bcm} + m_b + m_g + m_{gas}} \tag{16}$$

As the balloon ascends, it expands with altitude until it bursts at a maximum size due to the elastic properties of its material. The balloon's radius, modeled as a sphere, changes during ascent. While complex models account for heat exchange and pressure variation [21], in this paper we use a simpler model focusing only on material expansion due to pressure changes, employing the hyperelastic Mooney-Rivlin formula to capture the nonlinear behavior of the elastic material [22].

The absolute wind, on the other hand, is modeled in the Kalman filter's predictor as a constant, set to its initial value. This assumption, in the Kalman framework, is equivalent to setting the wind's predictor model as a constant-mean Gaussian process. We remark that the output of the filter estimate will *not* be a constant-mean Gaussian process: indeed, the filter will refine this estimation using actual sensor measurements as the posterior. This assumption leads to:

$$\ddot{\boldsymbol{x}}_{\boldsymbol{w}} = \mathbf{0} \tag{17}$$

Fig. 1 displays the absolute wind speed values derived from the Kalman filter over the first 250 seconds of the second flight.

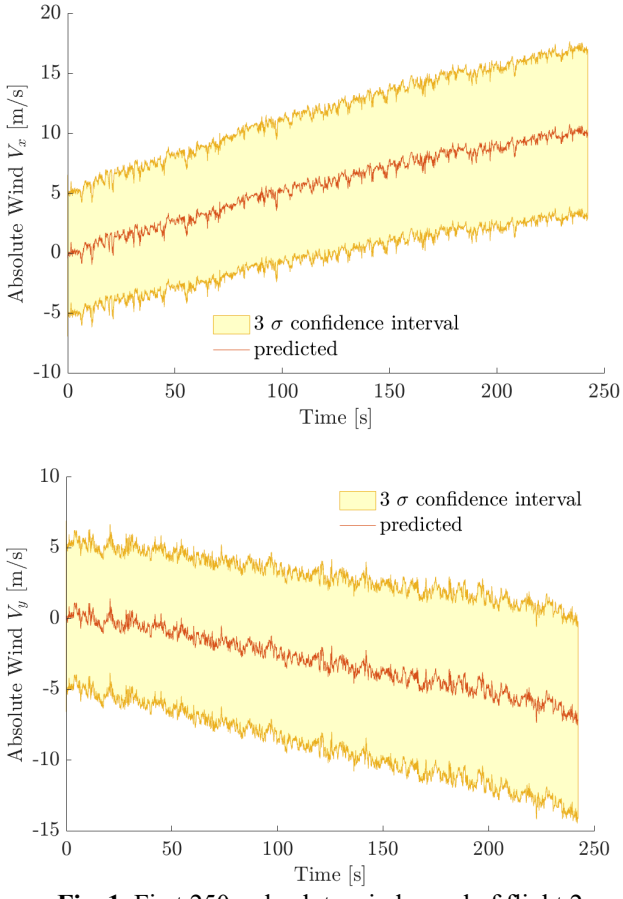

Fig. 1. First 250 s absolute wind speed of flight 2

6. Results

To validate the approach, we use the processed wind data of the second flight test. The selected part of the wind signal shown in Fig. 2 exhibits high variability, with a duration of over 10 minutes, peaks exceeding 8 m/s (around 16 knots), and variations exceeding 5 m/s (approximately 10 knots). This variability ensures that the method is tested against highly fluctuating gust conditions. The signal is the input of the wind model.

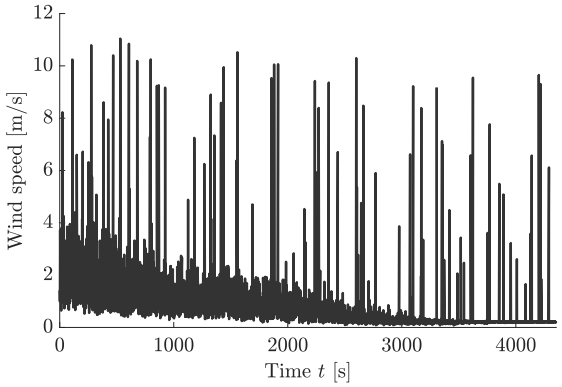

Fig. 2. Input wind speed signal

Initially, we evaluate the autocorrelation function of the signal. In this case, 100 lags are considered, meaning the signal is correlated with itself over the previous 100 seconds. The original ACF is then fitted with the superposition of equation of ACF of the SDE model in the form (11). A mixture of eight SDEs is used. The fitting step is used to determine the coefficient of the model, shown in Table 1. The coefficients are employed to construct the superposition of SDEs in the form (8).

Subsequently, the equation is integrated to obtain an initial synthetic signal with an autocorrelation function of the input data. As anticipated, the process still has a Gaussian probability density function, illustrated in Fig. 3. To impose the desired probability density function of the data to the signal generated from the integration of the SDE, we employ the memoryless transformation method, as previously outlined. The cumulative distribution function of the data is first evaluated, as illustrated in Fig. 4.

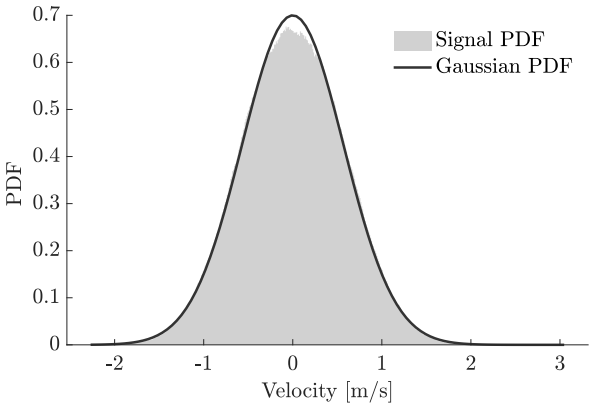

Fig. 3. Gaussian PDF of the synthetic signal

Parameter	Eq.1	Eq.2	Eq.3	Eq.4	Eq.5	Eq.6	Eq.7	Eq.8
α	0.5352	0.000046	0.00071	0.000031	0.99774	0.00011	0.00161	0.14205
σ	0.9346	12.4314	6.5272	12.3759	8.3983	6.2124	6.2831	12.1872
ω	0.0796	0.0097	0.0045	0.0072	0.1181	0.0169	0.7190	0.0447

Table 1. Model's coefficients

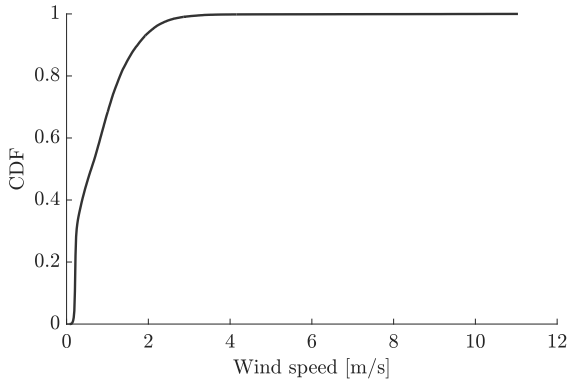

Fig. 4. CDF of data

Finally, we obtained the synthetic signal with the desired autocorrelation function and probability density function. The autocorrelation function and probability density function are the same as in the data, as shown in Fig. 5.

7. Conclusions

In this paper, we presented a robust framework for simulating wind gusts on Venus using a set of SDEs, specifically a bidimensional Ornstein-Uhlenbeck process. Our approach accurately captures the ACF and PDF of measured wind signals, crucial for simulating the behavior of a Venus aerobot under extreme wind conditions.

We tested our method using real-world wind speed data collected during flight tests in the Mojave Desert, demonstrating that the model can effectively replicate the statistical characteristics of wind speed measurements. The integration of an extended Kalman filter allowed for the precise processing of real-time wind signals, further enhancing the model's accuracy.

Our findings indicate that the proposed method not only simplifies implementation but also provides a reliable tool for simulating wind conditions, which is essential for the successful deployment and operation of aerobots on Venus. However, it is important to note that while this paper presents a method for constructing stochastic models, the utility of these models for Venusian conditions is currently limited by the absence of empirical wind data for the planet.

Future work will focus on refining the model to incorporate more complex wind patterns and extending its applicability to other planetary bodies with challenging atmospheric conditions. Additionally, further validation with a broader range of data sets and integration with real-time aerobot control systems will be pursued to enhance the practical utility of the model.

This research contributes significantly to the field of planetary exploration, offering a valuable tool for mission planning and execution in extreme environments.

Acknowledgements

This research was carried out at Jet Propulsion Laboratory, California Institute of Technology under a contract with the National Aeronautics and Space Administration (80NM0018D0004), as part of the JPL Visiting Student Research Program that hosted Ms. Bandinelli under the mentorship and supervision of Drs.

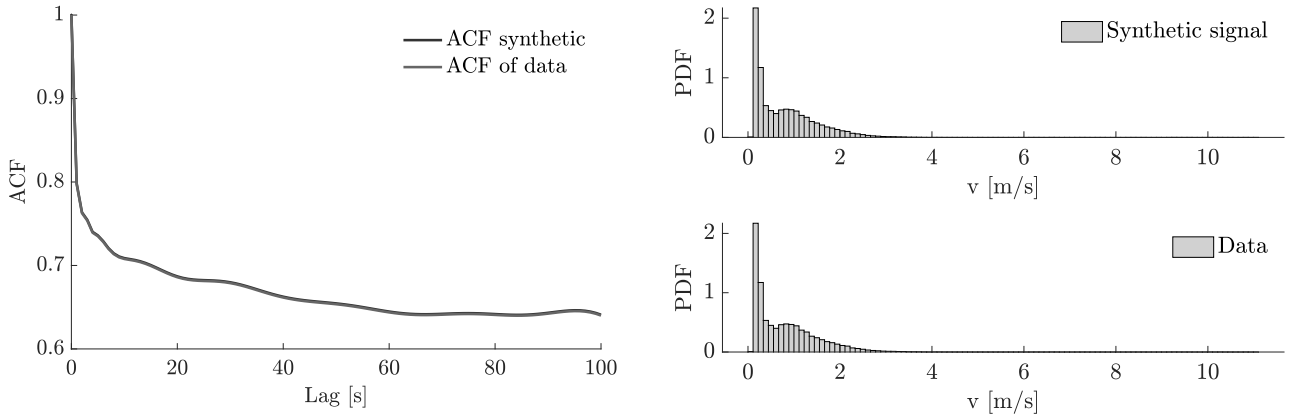

Fig. 5. The ACF and PDF of the data and of the simulated SDE model

Quadrelli and Rossi. The authors are grateful to Dr. James Cutts, Dr. Jacob Izraelevitz, Dr. Len Dorsky, and Dr. Richard Blomquist for useful discussions.

References

[1] L. R. Dartnell, Constraints on a potential aerial biosphere on Venus: I. Cosmic rays, Icarus 257 (2015) 396–405.
[2] National Academies of Sciences, E., Medicine, et al., Origins, Worlds, and Life: A Decadal Strategy for Planetary Science and Astrobiology 2023-2032, Washington, 2022.
[3] Venus Aerial Platforms Study Team, Aerial Platforms for the Scientific Exploration of Venus Summary Report. Tech. rep. Jet Propulsion Laboratoy, 2018.
[4] W. T. Huntress Jr., M. Ya Marov, Soviet Robots in the Solar System: Mission technologies and discoveries, Springer, 2011.
[5] S. Lebonnois, A. Sanchez Lavega, T. Imamura, Atmospheric Dynamics of Venus, Space Sci. (2017), 1541–1616.
[6] S. Lebonnois, F. Hourdin, V. Eymet, A. Crespin, R. Fournier, F. Forget, Superrotation of Venus' atmosphere analyzed with a full general circulation model, Journal of Geophysical Research: Planets 115 (2010).
[7] P. Scarica, I. Garate-Lopez, S. Lebonnois, G. Piccioni, D. Grassi, A. Migliorini, S. Tellmann, Validation of the IPSL Venus GCM thermal structure with Venus Express data, Atmosphere 10 (2019) 594.
[8] A. Sánchez-Lavega, et al., Variable winds on Venus mapped in three dimensions, Geophys. Res. Lett. (2008) 35.
[9] F. Rossi, M. Saboia, S. Krishnamoorthy, J.Vander Hook, Proximal exploration of Venus volcanism with teams of autonomous buoyancy-controlled balloons, Acta Astronautica 208 (2023) 389-406.
[10] M. Lei, L. Shiyan, J. Chuanwen, L. Hongling, Z. Yan, A review on the forecasting of wind speed and generated power, Renew. Sustain. Energy Rev. 13 (2009) 915-920.
[11] E. Erdem, J. Shi, ARMA based approaches for forecasting the tuple of wind speed and direction, Appl. Energy 88 (2011) 1405-1414.
[12] G. D'Amico, F. Petroni, F. Prattico, First and second order semi-Markov chains for wind speed modeling, Phys. Stat. Mech. Appl. 392 (2013) 1194-1201.
[13] A. Shamshad, M.A. Bawadi, W.M.A.W. Hussin, T.A. Majid, S.A.M. Sanusi, First and second order Markov chain models for synthetic generation of wind speed time series, Energy 30 (2005) 693-708.
[14] M. B. Quadrelli, J. M. Cameron, V. Kerzhanovich, Multibody Dynamics of Parachute and Balloon Flight Systems for Planetary Exploration, J. Guid. Con. And Dyn. 27 (2004) 564-571.
[15] B. Oksendal, Stochastic Differential Equations: An Introduction with Applications, Springer-Verlag, Berlin Heidelberg, 2010.
[16] S. Sarkka, A. Solin, Applied Stochastic Differential Equations, Cambridge University Press, 2019.
[17] P. E. Kloeden, E. Platen, Numerical Solution of Stochastic Differential Equations, Springer-Verlag, Berlin Heidelberg, 1992.
[18] G.E. Uhlenbeck, L.S. Ornstein, On the theory of the brownian motion, Physical Review 36 (1930) 823–842.
[19] G. Weinberg, L. Gunn, Simulation of Statistical Distributions using the Memoryless Nonlinear Transform, Technical rept. (2019).
[20] Y. Saito, T. Mitsui, Stability analysis of numerical schemes for stochastic differential equations, Numer. Anal. 33 (1996) 2254-2267.
[21] A. Gallice et al., Modeling the ascent of sounding balloons: derivation of the vertical air motion, Atmospheric Measurement Techniques 4.10 (2011) 2235–2253.
[22] I. Muller, P. Strehlow, Rubber and Rubber Balloons: Paradigms of Thermodynamics, Springer, 2004.